

Investigation of coupling geometry and dimerization effects on thermoelectric properties of a C_{60} molecular transistor

M. Bagheri Tagani, Z. Golsanamlou, S. Izadi, and H. Rahimpour Soleimani,
Department of physics, University of Guilan, P.O.Box 41335-1914, Rasht, Iran

June 25, 2021

Abstract

Thermoelectric properties of a C_{60} molecular transistor are studied using Green function formalism in linear response regime. A tight-binding model is used to investigate the effect of the dimerization and coupling geometry on the electrical conductance, thermopower, and figure of merit. Increase of the connection points between the molecule and electrodes results in decrease of the number of the peaks of the electrical conductance owing to the interference effects. In addition, oscillation of the thermopower is reduced by increase of the connection points. It is also observed that the kind of carriers participating in the energy transport is dependent on the coupling geometry. Results show that the increase of the connection points leads to the reduction of the figure of merit.

1 Introduction

Molecular junctions and quantum dots (QDs) have great potential for electronic, spintronic, and energy conversion applications. Discreteness of energy levels, strong Coulomb correlations, and interference effects result in the novel and interesting phenomena such as: negative differential conductance [1, 2, 3, 4], ratchet effect [5], spin and Coulomb blockade effects [6, 7, 8], and Kondo effect [9, 10, 11, 12]. Energy conversion to electricity is an important challenge which has become a hot topic in recent years because of the recent advances in manufacturing nanoscale devices. Strong quantum effects in such devices result in the violation of the Wiedemann-Franz law [13, 14]

and as a consequence, increase of the thermoelectric efficiency. The thermoelectric efficiency is described by a dimensionless quantity as figure of merit, $ZT = G_e S^2 T / \kappa$, where G_e and κ stand for the electrical and thermal conductances, respectively. S denotes the thermopower and T is the operating temperature. Unlike bulky samples, molecular devices can have the figure of merit higher than unity indicating they can work as good thermoelectric devices. The thermoelectric experiments can be also used to study the nature of the transport through molecules. For example, the positive thermopower shows that the transport is dominant by holes through the HOMO level, whereas the negative thermopower indicates the electron participation in the transport through the LUMO level.

The C_{60} molecule is consist of 12 pentagons and 20 hexagons. The energy gap of the molecule is about $2eV$ causing an insulator-like behavior in the room temperature [15]. The molecule can be used as a good conductive single molecular junction because of delocalization of the frontier orbitals of C_{60} . Therefore, a lot of research has been done on the transport properties of the C_{60} based devices experimentally and theoretically [16, 17, 18, 19, 20, 21, 22, 23, 24]. Park et al. [16] fabricated the first individual C_{60} molecular transistor. Their transport experiments revealed the coupling between the center of mass motion of the molecule and the electronic degrees of freedom and the step-like behavior of the current-voltage characteristic. Néel and co-workers [17, 18] studied the influence of the couplings on the conductance of a C_{60} molecular transistor and found that the decrease of the distance between the molecule and the scanning tunneling microscope tip results in the increase of the conductance. It has been shown that the C_{60} junctions can have high conductance if they are coupled to the proper electrodes [23].

Study of the thermoelectric properties of the molecular junctions has very recently gained a lot of attention from both experimental and theoretical points of view [24, 25, 26, 27, 28, 29, 30, 31, 32, 33, 34, 35, 36]. Tan and co-workers [28] studied the effect of length and contact chemistry on the thermoelectric properties of a molecular junction. They observed the asymmetry of the coupling strength between the molecule and electrodes results in the significant reduction of the electrical conductance, whereas the thermopower varied by only a few percent. The coupling strength was changed by switching the coupling chemistry. In addition, it was found that the thermopower linearly increases by increment of the molecule length. Very recently, thermal transport through carbon nanobuds has been investigated using Molecular dynamics simulations [36]. Results show that the nanobuds can be used as good thermal conductor. Balachandran et al. [33] found that end-group-mediated charge transfer between the molecule and electrodes plays an important role in the thermoelectric properties of triphenyl molecules.

Their results also show that the sign of the thermopower is related to the HOMO-LUMO energies. Bilan and co-workers [24] studied the conductance and thermopower of single-molecule junction based on a C_{60} molecule using the density functional theory within the nonequilibrium Green function technique. They found that the junction can be highly conductive and thermopower is negative because the lowest unoccupied molecular orbital dominates the charge transport.

In this article, the thermoelectric properties of a C_{60} transistor is investigated using Green function formalism in the linear response regime. The C_{60} can couple to the electrodes through a single point, a pentagon, or a hexagon. The kind of coupling can significantly affect the transport properties of the molecule as it was predicted in [21]. The kind of the coupling strongly influences on the transmission shape and with respect to the fact that the transmission coefficient is the most important parameter in the study of the thermopower in the linear response regime, therefore; the figure of merit of the C_{60} transistor is strongly dependent on the shape of the coupling. However, the effect of the coupling geometry and bond dimerization on the thermoelectric properties of a C_{60} has not been addressed so far. In the next section, a tight-binding model is used to describe the C_{60} and electrode Hamiltonian and the thermoelectric coefficients are presented by means of the Green function language. Sec. III is devoted to the numerical results. A brief conclusion is given in Sec. IV .

2 Model and Formalism

We consider a C_{60} molecule coupled to one dimensional metallic electrodes. The tight-binding approximation with only one orbital per atom is used to describe the molecule. The Hamiltonian is given by

$$H_{mol} = \sum_{i=1}^{60} (\varepsilon_i + eV_G) d_i^\dagger d_i - \sum_{\langle ij \rangle} t_{ij} d_i^\dagger d_j, \quad (1)$$

where ε_i is the on-site energy of the i th orbital taken as the zero of energy. V_G denotes the gate voltage used to control the energy levels of the molecule. d_i is the annihilation operator destroying an electron in the orbital i . t_{ij} is the hopping matrix element assumed to be nonzero only between nearest-neighbor orbitals $\langle ij \rangle$. Because the C_{60} is composed of the single and double bonds with different lengths, we set $t_1 = 2.5$ for single bonds and $t_2 = 1.1t_1$ for double bonds [37].

The electrodes are described as

$$H_C = \sum_{\alpha, i_\alpha} \varepsilon_{i_\alpha} c_{i_\alpha}^\dagger c_{i_\alpha} - \sum_{\alpha i_\alpha j_\alpha} t_{i_\alpha j_\alpha} c_{i_\alpha}^\dagger c_{j_\alpha}, \quad (2)$$

where $t_{i_\alpha j_\alpha} = t_1$ is the hopping matrix element of the electrode $\alpha = L, R$, and $\varepsilon_{i_\alpha} = 2t_{i_\alpha j_\alpha}$ is the on-site energy of the electrode. The coupling between the molecule and electrodes is given as

$$H_T = \sum_{\alpha i_\alpha j} (t'_\alpha c_{i_\alpha}^\dagger d_j + h.c.), \quad (3)$$

where $t'_\alpha = t_{i_\alpha j_\alpha}/2$ stands for the coupling strength. We assume that the spin is conserved during the tunneling from the electrodes to the molecule.

The retarded Green function of the molecule coupled to the electrodes is given as

$$G^r(\varepsilon, V_G) = [(\varepsilon + i0^+)I - H_{mol} - \Sigma_L(\varepsilon) - \Sigma_R(\varepsilon)]^{-1}, \quad (4)$$

where the couplings effect is taken into account by the self-energy functions, $\Sigma_\alpha(\varepsilon)$. ε denotes the energy of the injected electron from the leads, and 0^+ is an infinitesimal value. $\Sigma_\alpha(\varepsilon)$ describes the effect of the semi-infinite electrodes on the molecule and for one dimensional electrodes is given as [38]

$$\Sigma_\alpha(\varepsilon) = -t_\alpha'^2 g_\alpha(\varepsilon) = -\frac{t_\alpha'^2}{t} e^{ika}, \quad (5)$$

where $t = t_{i_\alpha j_\alpha}$, $ka = a \cos(1 - (\varepsilon - \varepsilon_\alpha)/2t)$, and $\varepsilon_\alpha = \varepsilon_{i_\alpha}$. The real part of the self-energy shifts the position of the energy levels of the molecule, whereas its imaginary part results in the broadening of the density of states of the molecule and the finite lifetime of the electron in the molecule. The coupling between the C_{60} and electrodes depends on the orientation of the molecule so that one carbon atom, a pentagon or a hexagon may couple to the electrodes. The coupling geometry significantly affects the self-energy matrix so that it has only one nonzero element for single atom connection, 25 nonzero elements for a pentagon and 36 nonzero elements for a hexagon coupling. The more details about the coupling geometry can be found in [21].

In order to compute the charge and heat currents, the Keldysh nonequilibrium Green function formalism is used. The charge and heat currents are given as follows [38, 39]

$$I = \frac{2e}{h} \int d\varepsilon [f_L(\varepsilon) - f_R(\varepsilon)] T(\varepsilon), \quad (6a)$$

$$Q = \frac{2}{h} \int d\varepsilon (\varepsilon - \mu_L) [f_L(\varepsilon) - f_R(\varepsilon)] T(\varepsilon), \quad (6b)$$

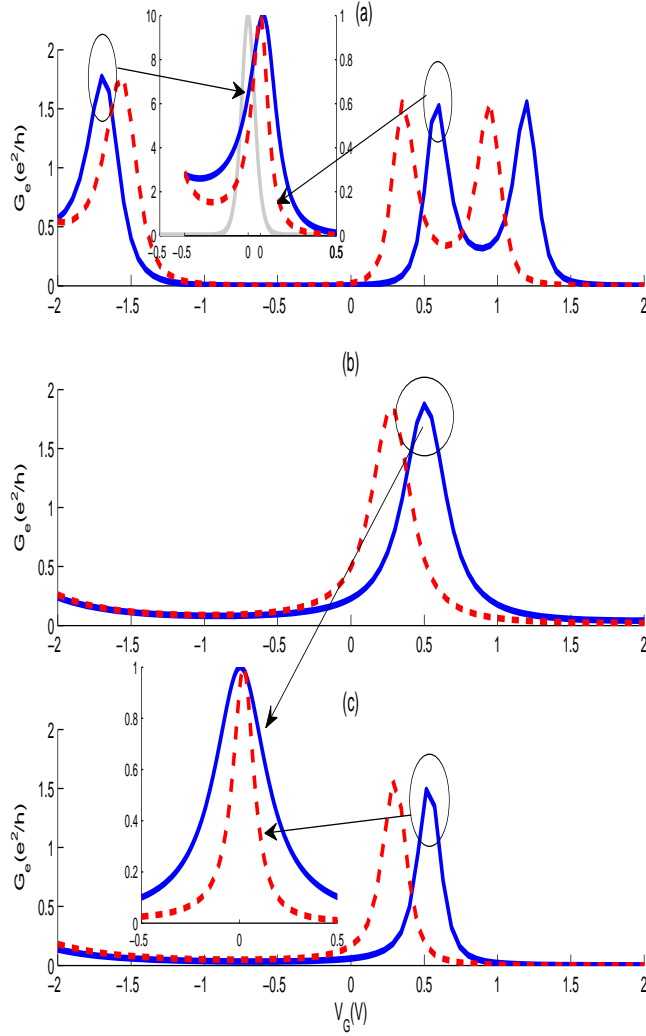


Figure 1: Electrical conductance (a) single point coupling, (b) five points coupling, and (c) six points coupling for $t_2 = t_1$ (solid line) and $t_2 = 1.1t_1$ (dashed line). Upper panel shows the transmission coefficient at $V_G = -1.7$ (solid) and $V_G = 1.5$ (dashed). The fermi derivative is plotted in gray. Lower panel shows the transmission coefficient of the five atom (solid) and six atom (dashed) connections for voltage gates indicated by circle.

where $f_\alpha(\varepsilon) = [1 + \exp((\varepsilon - \mu_\alpha)/kT_\alpha)]^{-1}$ is the Fermi distribution function of the electrode α , μ_α and T_α denote, respectively, the chemical potential and temperature of the electrode α . $T(\varepsilon) = \text{Tr}[\Gamma_L(\varepsilon)G^r(\varepsilon)\Gamma_R(\varepsilon)G^a(\varepsilon)]$ is the transmission coefficient and $\Gamma_\alpha = -2\text{Im}(\Sigma_\alpha)$ is the coupling matrix.

We investigate the thermoelectric properties of the C_{60} molecule in the linear response regime in which the charge and heat currents are expressed in terms of the applied temperature difference, ΔT , and induced voltage drop, ΔV , to first order according to

$$I = e^2 L_0 \Delta V + \frac{e}{T} L_1 \Delta T, \quad (7a)$$

$$Q = e L_1 \Delta V + \frac{1}{T} L_2 \Delta T, \quad (7b)$$

where L_n are integrals of the form

$$L_n = -\frac{1}{h} \int d\varepsilon (\varepsilon - \mu)^n \frac{\partial f}{\partial \varepsilon} T(\varepsilon), \quad (8)$$

where μ is the chemical potential of the leads in the equilibrium. Thermopower is the ratio of the voltage drop to the applied temperature difference under condition that the current vanishes $I = 0$, therefore, $S = -\frac{1}{eT} \frac{L_1}{L_0}$. The electrical, G_e , and thermal, κ , conductances are given as

$$G_e = e^2 L_0, \quad (9a)$$

$$\kappa = \frac{1}{T} [L_2 - \frac{L_1^2}{L_0}]. \quad (9b)$$

In the following, we analyze the dependence of the electrical and thermal conductances, thermopower and the figure of merit on the dimerization, coupling geometry and temperature. To compute the figure of merit, we neglect the lattice thermal conductance which is usually small in nanostructures.

3 Results and Discussion

Figure 1 shows the electrical conductance as a function of gate voltage for different coupling geometries. In single atom contact, the conductance peaks are exactly located at the molecular energy levels as it was expected. There are three peaks denoting HOMO, LUMO, and LUMO+1, respectively. The gap is about $2eV$ which is consistent with previous results. The dimerization affects HOMO and LUMO peaks in different manners so that the peak located at HOMO is shifted toward right, whereas the one located at LUMO

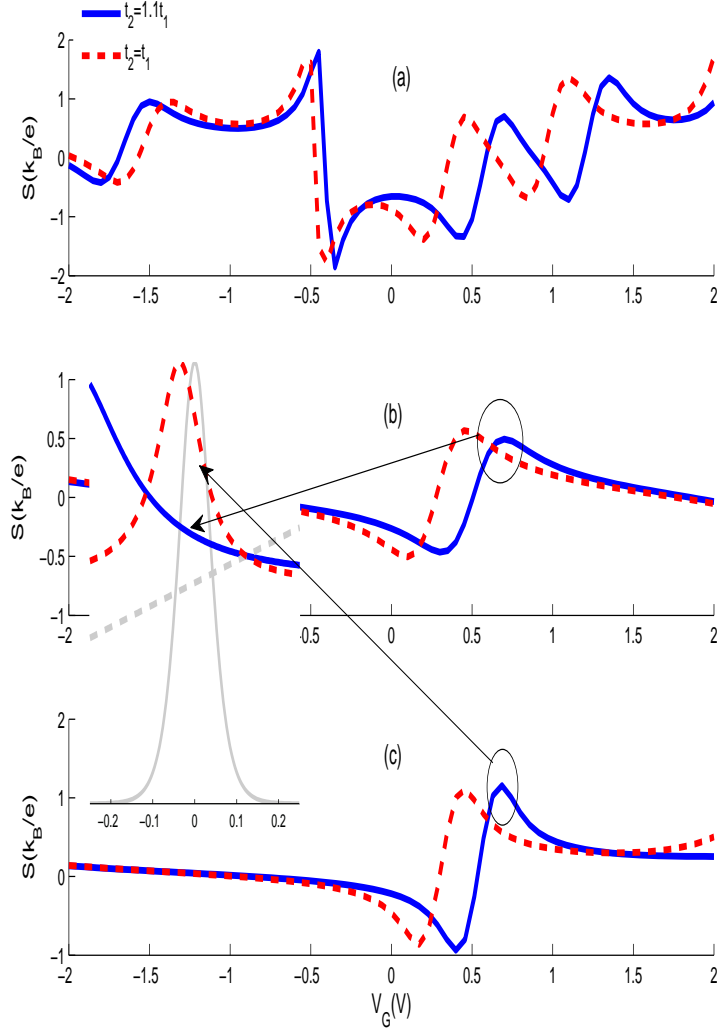


Figure 2: Thermopower versus gate voltage for (a) single atom connection, (b) five atom connections, and (c) six point connections at $t_2 = t_1$ (solid) and $t_2 = 1.1t_1$ (dashed). Inset shows the transmission function of the five point (solid) and six point (dashed) connections. The Fermi derivative and $\varepsilon - \mu$ are shown by gray solid and dashed lines, respectively. $T = 300K$.

is moved to the left when $t_1 = t_2$. The eigenvalues of Hamiltonian of the C_{60} are strongly dependent on t_1 , and t_2 , therefore, such change is predictable. Our analysis shows that the gap is reduced up to $0.35eV$ when $t_1 = t_2$. In addition, it is observed the peak located at HOMO is slightly higher than the ones located at LUMO and LUMO+1. With respect to the fact the electrical conductance is directly related to the transmission coefficient, the difference arises from the changes of the transmission. In the upper panel, we plot the transmission coefficient at $V_G = -1.7$, HOMO, and $V_G = 1.5$, LUMO. As it is observed the transmission is wider in the HOMO and the difference in the width of the transmission coefficient gives rise to the difference in the height of G_e .

Unlike single atom contact, the electrical conductance exhibits just one peak located at LUMO in the case of connection to five or six carbon atoms. The decrease of the number of the conductance peaks is a direct result of interference effects. In fact, with increase of the crossing channels for injection of electrons from electrodes to the molecule, the electron waves may suffer a destructive or constructive interference. The destructive interference leads to the vanishing of the transmission peaks and as a result, the electrical conductance peaks are disappeared. Moreover, it is observed that the position of the peak in five or six atom connections is slightly different from the single atom connection. The difference comes from the real part of the self energy. Real part of self energy shifts the molecular energy levels and such shift becomes more pronounced with increase of connection points. As single point case, the peak is moved toward left when $t_1 = t_2$, however, the height of peak is constant. In addition, it is observed that the electrical conductance has higher peak in five point connections because the transmission coefficient is wider in five point connections, see lower panel.

The dependence of thermopower on gate voltage is plotted in Fig. 2. The change of the electron population of the molecule results in the oscillation of the thermopower which has been extensively reported for the quantum dots and molecules [40, 41, 42]. The sign of the thermopower determines the kind of the carrier responsible for the transfer of the current and energy. In the single point contact, the thermopower has five zeros which three of them are located at resonance energies and others are in the electron-hole symmetry points. The thermopower varies sharper in the symmetry points. In the resonance energies the thermopower is zero because the temperature difference cannot induce a net current. In fact, electrons can tunnel from the hotter and colder electrodes to the molecule without needing to the thermal energy. In symmetry points, electrons and holes participate in the transfer of charge and energy with the same weight. Electrons and holes carry the charge in the opposite directions so the net current is zero. In this points,

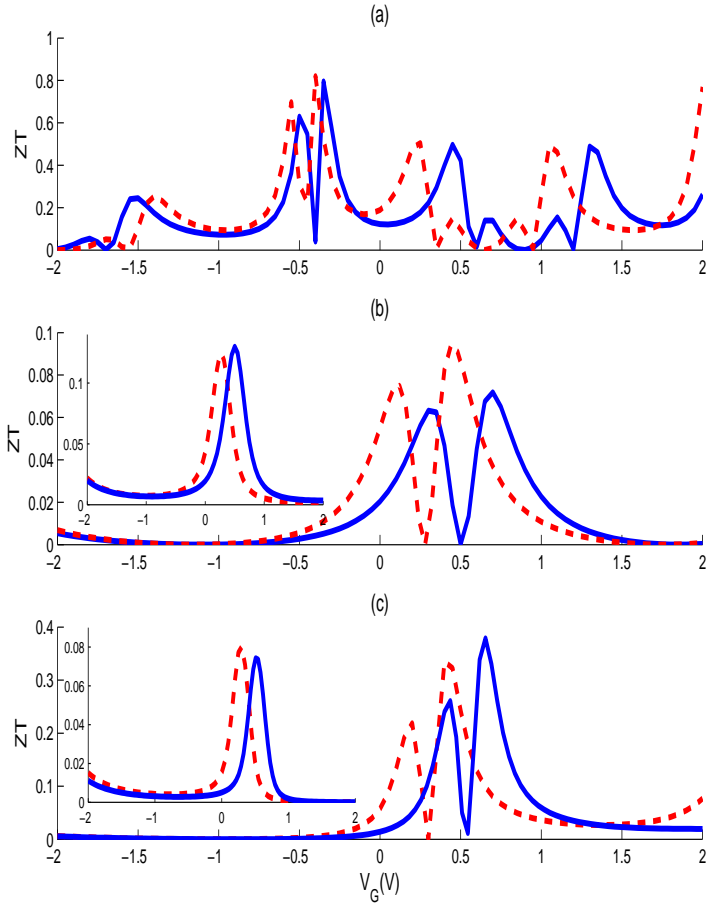


Figure 3: ZT versus gate voltage in (a) single atom, (b) five atom and (c) six atom connections for $t_2 = t_1$ (solid) and $t_2 = 1.1t_1$ (dashed). Upper panel shows the thermal conductance of the five point connections case, while the lower panel shows the thermal conductance of the six atom connections.

the thermal conductance is maximum because they carry the energy in the same direction. The sign of the thermopower changes in the vicinity of the resonance and symmetry energies. For gate voltages lesser than resonance, the thermopower is positive (note that the thermopower in the unit of k_B/e is negative due to negative electron charge.) indicating the electrons of the hotter lead carry the current, whereas for gate voltages lesser than symmetry energies, the thermopower is negative because the holes carry the current. Such behavior was previously reported for systems composed of single and double QDs [41, 43]. It is interesting to note that the thermopower is asymmetry because of the electron-hole symmetries. The dimerization changes the position of the resonance and symmetry points. In addition, the magnitude of the thermopower slightly changed.

The increase of the connection points significantly reduces the oscillation of the thermopower. It comes from the fact that the lesser molecular energy levels are involved in the thermoelectric transport due to the destructive interference effects. Results show that the magnitude of the thermopower is more in the six point contacts than the five point contacts. The difference is a direct result of the change of the transmission in the vicinity of the chemical potential of the electrodes. As it is shown in the inset, the transmission coefficient of the six point contact is more in the range of $\partial f/\partial \varepsilon$, therefore, L_1 increases and as a consequence, the thermopower is increased.

Figure 3 shows the figure of merit as a function of gate voltage for different coupling geometries. In single point connection, ZT has a lot of peaks with significant magnitudes in a wide range of the gate voltage. Increase of the number of connection points results in the decrease of the number of peaks. This reduction results from the destructive interference previously discussed. The change of the strength of the bonding does not affect the magnitude of the ZT and just changes the position of the peaks. In the five and six point connections, the dimerization influences on the magnitude of the ZT . In five point connections, the figure of merit increases when $t_2 > t_1$ owing to the increase of the thermopower and the decrease of the thermal conductance. The thermal conductance of the five point connections is plotted in the upper panel. It is so interesting to note that the ZT of the six point connections is increased when $t_1 = t_2$. In this case, although the thermopower is slightly decreased, the electrical and thermal conductances are increased with different rates so that the figure of merit is enhanced. The behavior of the thermal conductance of the six point connections is plotted in the lower panel.

Dependence of the thermoelectric coefficients on the temperature is plotted in Fig. 4. We set $V_G = 0.3V$. As it is observed the coupling geometry strongly affects the coefficients. The increase of temperature results in the broadening of the Fermi derivative and increase of the electron population

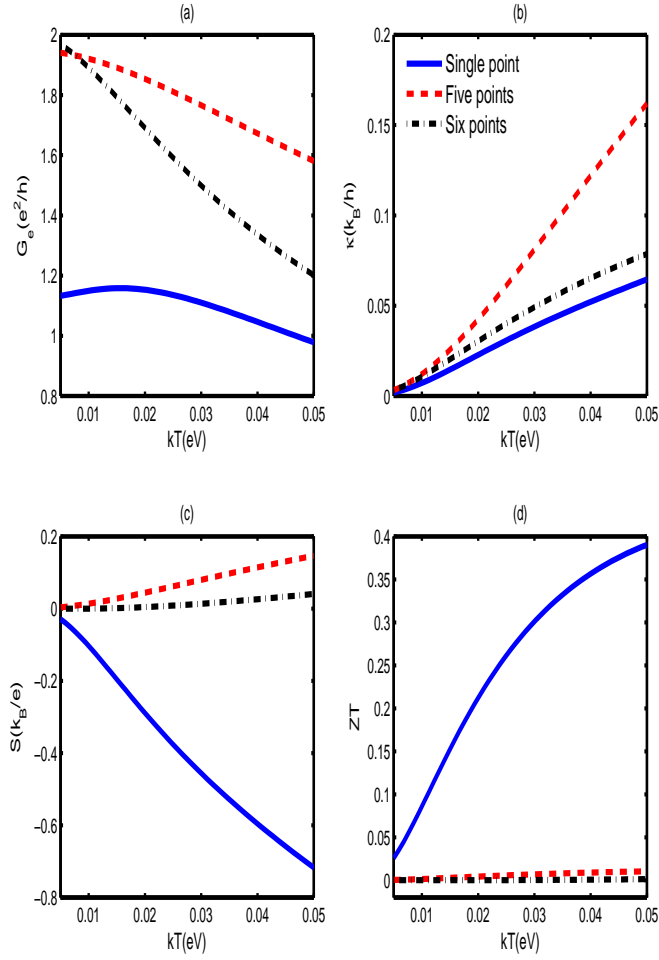


Figure 4: (a) Electrical conductance, (b) thermal conductance, (c) thermopower, and (d) figure of merit against temperature.

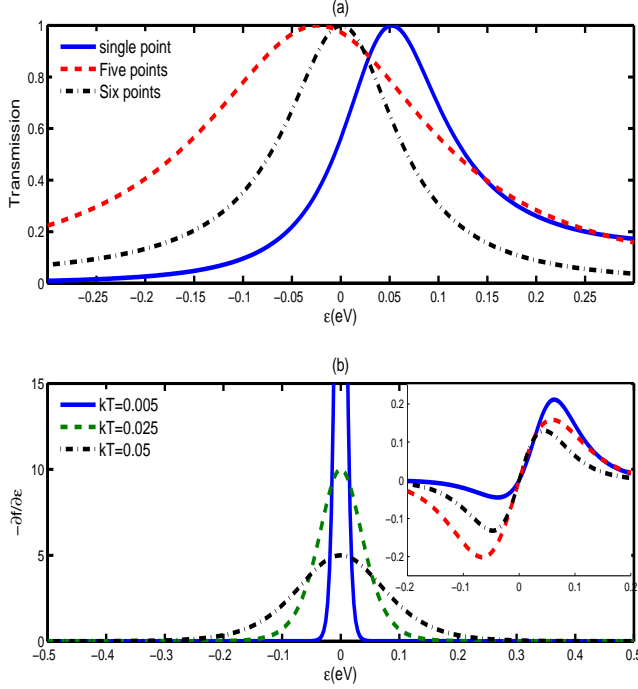


Figure 5: (a) Transmission coefficient and (b) Fermi derivative versus energy. Inset shows $T(\epsilon)(\epsilon - \mu)f'(\epsilon)$

in the molecule, nevertheless, the transmission coefficient is independent of temperature. It is worth noting that the Green function becomes a function of the electron density if the Coulomb correlations are taken into account. Fig. 5a and b shows the transmission coefficients for different coupling geometries and the Fermi derivative for different temperatures, respectively. The transmission coefficient is a Lorentz-like function in the vicinity of the chemical potential of the electrodes, see Fig. 5a, whose center and width are related to the coupling geometry. The center of the transmission coefficient of the six point connections is exactly located at the Fermi energy, therefore, its electrical conductance is more than others in low temperatures. With increase of temperature, the electrical conductance of the five point connections is more than others because its transmission coefficient is wider. The electrical conductance of the five and six point connections is monotonically decreased by increase of temperature because of the reduction of the height of the Fermi derivative. The dependence of the electrical conductance of single point on the temperature is non-uniform so that first, it increases and then decreases. The initial increase comes from the fact that the center

of the transmission coefficient is slightly far from the Fermi energy, therefore, the increase of temperature brings more parts of the transmission in the nonzero energy of the Fermi derivative. The increase of temperature significantly reduces the height of the Fermi derivative, see Fig. 5b, so the electrical conductance decreases in high temperatures. Results show that the thermal conductance increases with increase of the temperature because the carriers convey more thermal energy. The increase is more remarkable in the five point connections resulting more broadening of the transmission in this case.

Fig. 4c shows the thermopower versus temperature. It is so interesting that the kind of carriers participating in the thermoelectric transport is different for single and multi couplings. In single point connection, electrons participate in the transport of the current and heat flux while the holes play the main role in multi couplings. It occurs due to the shape and more specially, the position of the center of the transmission peak. The center of peak is in positive energies for single point, therefore, electrons thermally excited and above the chemical potential of the leads can tunnel through the molecule. In five and six point connections, the center is in negative energies, therefore, more holes below the Fermi energy of the leads can enter the molecule. In addition, the magnitude of the thermopower in single point is much more other cases owing to the more energy distance of the center of the transmission from the Fermi energy. For more clarity, we plot $T(\varepsilon)(\varepsilon - \mu)f'(\varepsilon)$ in the Inset of the Fig. 5. One can see that this quantity is asymmetric around the Fermi energy so that, its positive part is more in single point and its negative part is more in other cases. The figure of merit is plotted in Fig. 4d. The thermopower is the more important quantity for the ZT , therefore, although the electrical conductance reduces in the single point connection, the figure of merit significantly increases because of the magnitude of the thermopower. Increase of temperature results in the increase of the figure of merit because the magnitude of the thermopower is enhanced with increase of kT .

4 Summary

In this article, we have analyzed the thermoelectric properties of a C_{60} molecular transistor in the linear response regime. A tight-binding model within the Green function formalism is used to compute the electrical conductance, thermopower, and figure of merit. Results show that the coupling geometry strongly control the thermoelectric properties of the device. Increase of the number of coupling points results in the decrease of the oscillation of the

thermopower, and decrease of the figure of merit. It is a direct result of the interference effects. In addition, the kind of the carriers participating in the thermoelectric transport is dependent on the coupling geometry and temperature.

References

- [1] L. Luo , D. A. Holden , W-J. Lan , and H. S. White, *ACS Nano*, **6** (7), 6507 (2012).
- [2] I. Weymann, J. Barnas', and S. Krompievski, *Phys. Rev. B* **85**, 205306 (2012).
- [3] H. Xie, Q. Wang, B. Chang, H. Jiao, and J.-Q. Liang, *J. Appl. Phys.* **111**, 063707 (2012).
- [4] S. Lee, Y. Lee, E. B. Song, K. L. Wang, and T. Hiramoto, *Appl. Phys. Lett.* **102**, 083504 (2013).
- [5] D. M.-T. Kuo, S-Y. Shiau, and Y-c. Chang, *Phys. Rev. B* **84**, 245303 (2011).
- [6] I. Weymann, B. R. Bulka, and J. Barnas', *Phys. Rev. B* **83**, 195302 (2011).
- [7] C-Yu Hsieh, Y-P. Shim, and P. Hawrylak, *Phys. Rev. B* **85**, 085309 (2012).
- [8] H. Ishida, and A. Liebsch, *Phys. Rev. B* **86**, 205115 (2012).
- [9] E. Mnnoz, C. J. Bolech, and S. Kirchner, *Phys. Rev. Lett.* **110**, 016601 (2013).
- [10] Rok Žitko, J. S. Lim, R. López, J. Martinek, and P. Simon, *Phys. Rev. Lett.* **108**, 166605 (2012).
- [11] S. J. Chorley, M. R. Galpin, F. W. Jayatilaka, C. G. Smith, D. E. Logan, and M. R. Buitelaar, *Phys. Rev. Lett.* **109**, 156804 (2012).
- [12] P. Tröster¹, P. Schmitteckert, and F. Evers, *Phys. Rev. B* **85**, 115409 (2012).
- [13] B. Kubala, J. König, and J. Pekola, *Phys. Rev. Lett.* **100**, 066801 (2008).

- [14] A. Garg, D. Rasch, E. Shimshoni, and A. Rosch, *Phys. Rev. Lett.* **103**, 096402 (2009).
- [15] *Science of Fullerenes and Carbon Nanotubes*, edited by M. S. Dresselhaus, G. Dresselhaus, and P. C. Eklund (Academic, New York, 1996).
- [16] H. Park, J. Park, A. K. L. Lim, E. H. Anderson, A. P. Alivisatos, and P. L. McEuen, *Nature* (London) **407**, 57 (2000).
- [17] N. Néel, J. Kröger, L. Limot, and R. Berndt, *Nanotechnology* **18**, 044027 (2007).
- [18] N. Néel, J. Kröger, L. Limot, T. Frederiksen, M. Brandbyge, and R. Berndt, *Phys. Rev. Lett.* **98**, 065502 (2007).
- [19] K. Yoshida, I. Hamada, S. Sakata, A. Umeno, M. Tsukada, and K. Hirakawa, *Nano Lett.* **13**, 481 (2013).
- [20] J. J. Palacios, A. J. Pérez-Jiménez, E. Louis, and J. A. Vergés, *Nanotechnology* **12**, 160 (2001).
- [21] A. Saffarzadeh, *J. Appl. Phys.* **103**, 083705 (2008).
- [22] S. Ulstrup, T. Frederiksen, and M. Brandbyge, *Phys. Rev. B* **86**, 245417 (2012).
- [23] M. Kiguchi, *Appl. Phys. Lett.* **95**, 073301 (2009).
- [24] S. Bilan, L. A. Zotti, F. Pauly, and J. C. Cuevas, *Phys. Rev. B* **85**, 205403 (2012).
- [25] S-H. Ke, W. Yang, S. Curtarolo, and H. U. Baranger, *Nano Lett.* **9**, 1011 (2009).
- [26] Y-S. Liu, B. C. Hsu, and Y-C. Chen, *J. Phys. Chem. C* **115**, 6111 (2011).
- [27] X. J. Tan, H. J. Liu, Y. W. Wen, H. Y. Lv, L. Pan, J. Shi, and X. F. Tang, *J. Phys. Chem. C* **115**, 21996 (2011).
- [28] A. Tan, J. Balachandran, S. Sadat, V. Gavini, B. D. Dunietz, S-Y. Jang, P. Reddy, *J. Am. Chem. Soc.* **133** (23), 8838 (2011).
- [29] B. C. Hsu, Y-S. Liu, S. H. Lin, and Y-C. Chen, *Phys. Rev. B* **83**, 041404(R) (2011).

- [30] J-W. Jiang, and J-S. Wang, *J. Appl. Phys.* **110**, 124319 (2011).
- [31] V. D. Blank, S. G. Buga, V. A. Kulbachinskii, V. G. Kytin, V. V. Medvedev, M. Yu. Popov, P. B. Stepanov, and V. F. Skok, *Phys. Rev. B* **86**, 075426 (2012).
- [32] A. Popescu, and P. M. Haney, *Phys. Rev. B* **86**, 155452 (2012).
- [33] J. Balachandran, P. Reddy, B. D. Dunietz, and V. Gavini, *J. Phys. Chem. Lett.* **3**, 1962 (2012).
- [34] Y. Asai, *J. Phys.: Condens. Matter* **25**, 155305 (2013).
- [35] C. Evangeli, K. Gillemot, E. Leary, M. T. González, G. Rubio-Bollinger, C.J. Lambert, and N. Agraït, *Nano Lett.* **13** (5), 2141 (2013).
- [36] G. C. Loh, and D. Baillargeat, *J. Appl. Phys.* **113**, 123504 (2013).
- [37] E. Manousakis, *Phys. Rev. B* **44**, 10991 (1991).
- [38] S. Datta, *Quantum Transport: Atom to Transistor* (Cambridge University Press, Cambridge, 2005).
- [39] Y. Meir, and N. S. Wingreen, *Phys. Rev. Lett.* **68**, 2512 (1992).
- [40] C. W. J. Beenakker, and A. A. M. Staring, *Phys. Rev. B* **46**, 9667 (1992).
- [41] M. B. Tagani, and H. R. Soleimani, *J. Appl. Phys.* **112**, 103719 (2012).
- [42] M. B. Tagani, and H. R. Soleimani, *J. Appl. Phys.* **113**, 143709 (2013).
- [43] M. B. Tagani, and H. R. Soleimani, *Solid State Commun.* **152**, 914 (2012).